SMAR 2019 – Fifth Conference on Smart Monitoring,
Assessment and Rehabilitation of Civil Structures

SMAR 2019

Shear strengthening using external Fe-SMA strips

Luis Alberto MONTOYA-CORONADO [1], Joaquín G. RUIZ-PINILLA [1], Carlos RIBAS [1], Antoni CLADERA [1]

[1] University of Balearic Islands, Palma (Balearic Islands), Spain

Contact e-mail: antoni.cladera@uib.es

ABSTRACT: New Fe-based shape memory alloys (Fe-SMA) have been developed during last years, and on-going research shows that they may become a competitive material for civil engineering applications due to their low cost in comparison to other shape memory alloys, their mechanical properties and corrosion resistance. The main highlighted property of the Fe-SMA used is the ability to recover around 1 % of its shape by heating it up to 160 ºC after being previously deformed. More importantly, bars and strips made of Fe-SMA can be used to prestress concrete members if the free recovery of the SMA element is restrained, obtaining recovery stresses upon 350 MPa. In this communication, a comprehensive characterization of a commercially available Fe-SMA strip will be presented. The Fe-SMA strips have been used to externally retrofit small scale beams without shear reinforcement. The paper will present the different behavior of the reference beams (without shear reinforcement), the retrofitted beams (with the activated strips fully wrapping the beams, generating recovery stresses) and with beams with the externally placed strips but without activation. The retrofitted beams with activated strips failed on bending, with a clear delay on the apparition of the shear cracks, meanwhile the reference beams failed on shear.

1 INTRODUCTION

Structural design is currently focused on performance-based design methods in order to optimize and control the failure mechanism of structures. This aspect has led to study and control the flexural behavior, by increasing specially its sectional ductility, and developing all sectional capacity in reinforced concrete structures. However, shear failures are brittle and, consequently, this type of failure should always be avoided, especially when a structure is subjected to high intensity seismic loading. For example, after the 2011 earthquake in Lorca (Spain), it was reported that in many cases, the lack of sufficient reinforcement in columns gave rise to failure through shear stresses and that this failure should have been avoided due to its brittle behavior (Ruiz-Pinilla et. al, 2016). References are made to similar cases in the earthquake in L'Aquila, Italy, in 2009 (Augenti and Parisi, 2014). Many different technologies to retrofit concrete structures and to increase their shear strength have been proposed with different materials. However, most of those technologies are passive: external strengthening will start working after an increment of deformation of the structural element.

Most SMAs have a high ductile behavior, or high energy dissipation capacity, which it is an important aspect on seismic or dynamic loading. Another important property is the Shape Memory Effect (SME): the prestrained material is capable to recover its initial shape with practically zero remaining strain after being heated, and cooled afterwards, to a predefined temperature. This latter effect presents a singular application when the free strain is restrained:

the SMA produces recovery stresses (Cladera et al., 2014). Those stresses produced by the SMAs may be used in civil engineering applications as prestressing forces. This communication will present the application of Fe-SMA strips as external reinforcement on small-scale beam specimens. The alloy used has similar chemical composition than conventional stainless steels, Fe–17Mn–5Si–10Cr–4Ni–1(V, C) (mass%) (Dong et al., 2009), whereby its corrosion resistance is expected to be comparable. The alloy will be activated at only 160 ºC, to avoid damaging the concrete. This Fe-SMA is more cost competitive than other SMAs (Ni-Ti or Ni-Ti-Nb) to be implemented in common cases in civil engineering applications (Shahverdi et al., 2016). Even though the super-elasticity is not present in this low-cost alloy, the high ductility and recovery shape is still present. In any case, the shape recovery capacity is lower than in other SMAs, only around 1%. However, this alloy can generate recovery stresses up to 350 MPa when the free recovery is impeded.

2 FE-SMA CHARACTERIZATION

In the experimental campaign reported in this communication 50 mm width and 0.5 mm thick strips are used. The material was received in austenite phase (γ) without prestraining. The production process of the Fe-SMA used is detailed in (Czaderski et al., 2014). A material characterization procedure was carried out to understand its thermo-mechanical behavior. The results show close agreement with the work of (Lee et al., 2013), who obtained an optimum value of prestraining up to 4% with residual elastic deformation of 3.1%.

Figure 1 shows an image of the pre-straining and stress-recovery tests performed at the University of Balearic Islands. Fig. 2 shows the stress-strain curves for a pre-straining test up to 4% (loading and unloading, in red) and a tensile monotonic test until failure. It can be observed the high ductility of this material, capable to achieve 40% of plastic strain. The remaining deformation after prestraining is also illustrated. Numerous cyclic tests (loading and unloading) were performed (approx. 80 tests). The mean modulus of elasticity is near to 194 GPa (Figure 3), computed between 100 and 300 MPa. The mean yield stress obtained using the off-set method is approximately 476 MPa (Figure 3). Moreover, the modulus of elasticity decreases in each cycle, converging around 100 GPA for very high strains (around 20%) in austenite phase (Figure 4). Figure 5 shows a complete test including initial prestraining (in blue in Fig. 5 and 6), followed by the stress recovery test during the activation under constrained strain and a monotonic test up to failure. The recovery stresses reached 351 MPa which was consistent with the result of the previously mentioned work. The modulus of elasticity at the beginning of the monotonic test after the activation was approximately 34 GPA (Fig. 5). This will be the elastic modulus to take into account in a real situation after retrofitting the beams and activating the strips. Figure 6 shows the stress-temperature curve during the activation of the sample. The stress increases as the temperature increases, due to the reverse martensitic transformation. During the cooling process, the recovery stresses keep increasing, due to the thermal contraction.

3 EXPERIMENTAL CAMPAIGN ON SMALL-SCALE RC BEAMS

Preliminary results of the experimental tests of six small-scale concrete beams are shown. A summary of the beam specimens is shown in Table 1. Two specimens were tested without any kind of shear reinforcement (R1 and R2, reference beams). The other four beams were strengthened with external Fe-SMA strips: two of them without activation (SP1 and SP2) and the last two tests were strengthened and the SMA was activated before testing (SA1 and SA2).

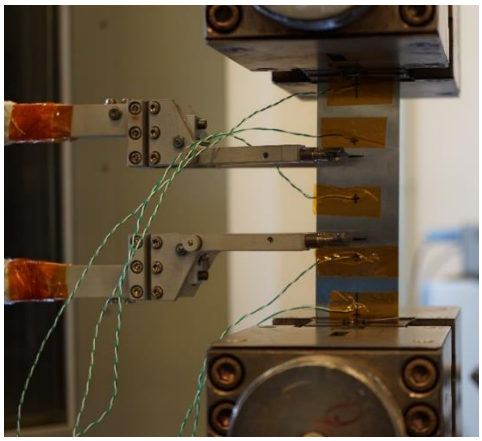

Figure 1. Fe-SMA characterization test set-up.

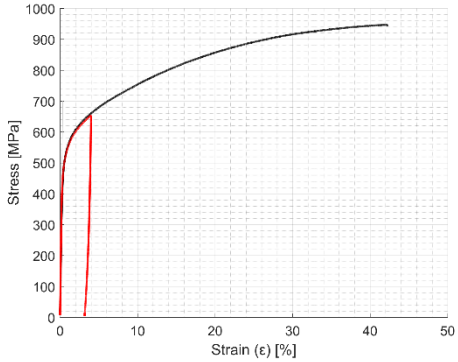

Figure 2. Monotonic and pre-straining test (4 %).

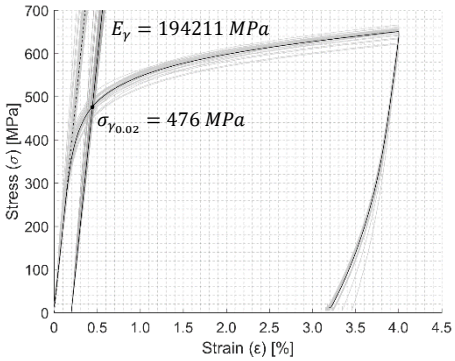

Figure 3. Average curves of 80 prestraining tests.

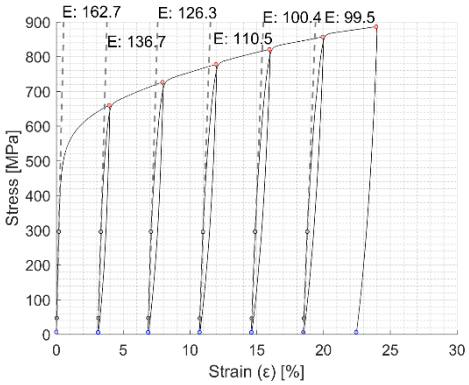

Figure 4. Decreasing of the modulus of elasticity, E.

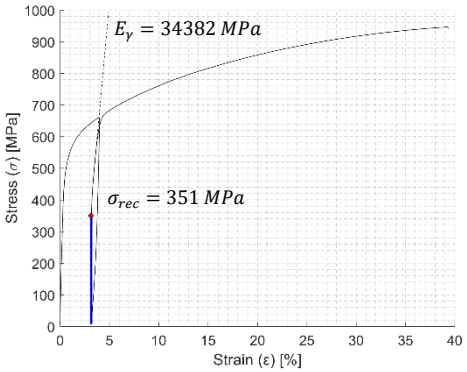

Figure 5. Complete test of prestraining, stress recovery and monotonic test up to failure.

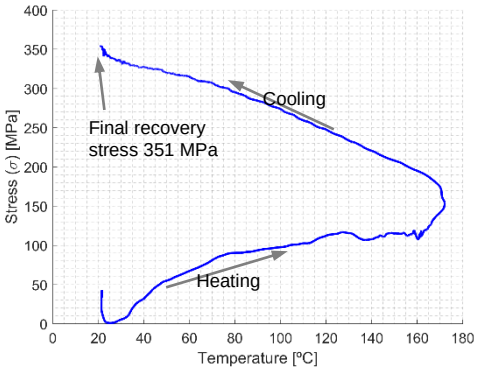

Figure 6. Stress -temperature curve during activation.

All the beams were tested with a three-point bending test scheme with a free span of 700 mm (Fig. 7). The cross section of the beam is a rectangular shape of 150 mm height, and 80 mm width. The total length of the beam specimens is 900 mm (Figure 7). Maximum aggregate size of 14 mm was used. Standard 150 mm cubes and 150 × 300 mm cylinders were cast with the specimens to obtain the mean compressive strength, f_{cm}, and the splitting strength, f_{ctm}, respectively. The mean $f_{cm(28)}$ and $f_{ctm(28)}$ at 28 days achieved were 23 MPa and 2.5 MPa, respectively. The concrete strength at the age of the tests of the beams is shown in Table 1.

Table 1. Detail of the beam specimen and test

Beam designation	Age at testing (days)	f_{cm} (MPa)	f_{ctm} (MPa)	Strip spacing (mm)	Strip width (mm)	Fe-SMA state	Comment
R1	172	30.1	2.8	-	-	-	Shear failure
R2	172	30.1	2.8	-	-	-	Shear failure
SP1	173	30.1	2.8	88.9	25	As provided	Mix-failure
SP2	173	30.1	2.8	88.9	25	As provided	Mix-failure
SA1	174	30.1	2.8	88.9	25	Activated	Mix-failure
SA2	175	30.1	2.8	88.9	25	Activated	Mix-failure

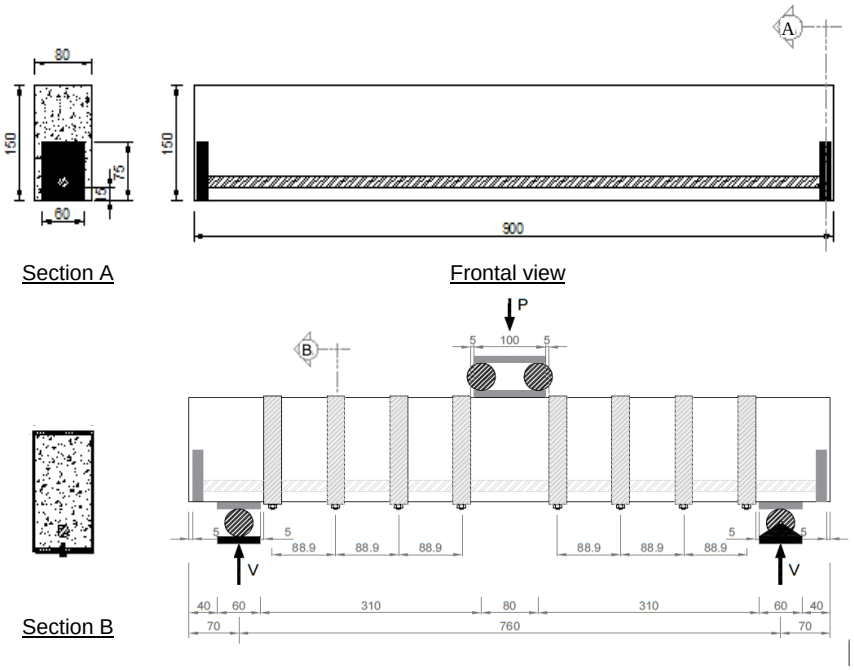

Figure 7. Specimen geometry and retrofitting layout

The longitudinal reinforcement is composed of a 16 mm (Ø16) standard B500SD rebar (A_s = 201 mm^2). Both ends of the rebar were welded to a plate to guarantee sufficient anchorage in such small specimens. The mechanical properties of the longitudinal bars are: f_y = 550 MPa, f_u = 649 MPa, ε_u = 27% (mean value).

The external shear strengthening was executed by 25 mm-width and 0.5 mm-thick Fe-SMA strips wrapping the beam with a slightly manual prestraining, using a strip tensor, to avoid gaps by ensuring the total contact between the strips and the beam. After the slight prestain, the strips were mechanically fixed to the beam (see Figure 7).

The activation of the Fe-SMA is achieved by reaching certain temperature through a heat-gun. The temperature is measured by means of numerous thermocouples on the strip ensuring to reach in all points 160 ºC. This temperature is necessary on the Fe-SMA to reach recovery stresses of 350 MPa in the case of a fully constrained strip. The load is applied by displacement control in the central zone of the specimen being the shear force in each support a half of the total load applied by the actuator.

4 EXPERIMENTAL RESULTS

It should be highlighted the initial difference that exists on the non-active and the active strips. If the strip is not totally fitted to the beam, and there are some gaps between the concrete and the strips, at the activation the strip will experience free recovery until it makes a total contact to the beam. After the full contact, prestressing forces will appear, confining the cross section of the element thanks to the recovery stresses. Figure 8 shows the gaps of a not-correctly placed strip and the beam. Those gaps are reduced after the activation of the strips.

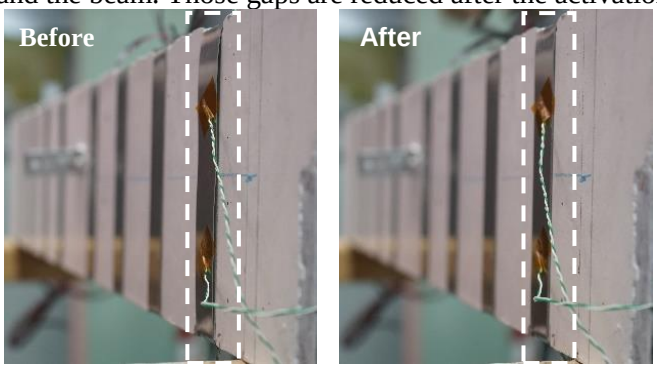

Figure 8. Comparison of the closing gap after activation of the Fe-SMA strips.

Figure 9 presents the shear force-maximum deflection curves for the six reported tests. Some representative values of each test are summarized in Table 2. It is observed that the all couple tests have a similar response to each other: R1/R2, SP1/SP2 and SA1/SA2. In the case of the reference beams (R1 and R2), there is a slightly difference on the fragility at failure, as failure was achieved very fast. After the shear crack appearance on the beam R1 a possible arch effect was developed which contribute for a slightly increment of the ultimate shear resistance.

The reference specimens (R1 and R2) reached a maximum shear force of 17.95 and 15.83 kN, respectively, while the strengthening specimen without activation (SP1 and SP2) reached values of 29.51 and 31.01 kN. The last two tests (strengthened and activated), SA1 and SA2, reached 31.68 and 31.64 kN, respectively. The strengthened and activated specimens achieved to hold a slightly higher load than the strengthened but not activated specimens, in both cases the shear capacity doubled the strength of the reference beams. In any case, the four strengthened beams (SP1, SP2, SA1 and SA2) failed on bending. It should be highlighted the stiffer behavior of SA1 and SA2 beams in comparison with SP1 and SP2 beams. The beams with the activated strips (SA1 and SA2) presented, at maximum load, a mid-span displacement equal to 6.52 and 5.83 mm. Non activated beams SP1 and SP2 presented, at maximum load, mid-span displacements of 7.89 and 9.34 mm. The activation of the strengthening strips generates confining stresses on the beam cross section, helping to obtain a better contact between the concrete and the SMA strips. For that reason, in the force-deflection curves, specimens SA1 and SA2 present a smooth behavior while on tests SP1 and SP2 there are oscillations on the results due to the presence of cracks before the non-activated strips are in full contact with concrete.

Figure 10 to Figure 12 show the state of the specimens when the maximum load is achieved. There are two images for each test merged together, left and right side of the beam. Crack patterns can be easily appreciated in each case thanks to the Digital Image Correlation (DIC). For each pair of tests, the crack patters of one beam is presented as the results of the DIC process, in order to show all cracks. Otherwise, only the thicker and principal cracks are appreciated (second beam of each pair).

Table 2. Summary of experimental results

Reference	Results		
	V_{max} (kN)	δ (mm)	$\delta_{85\%}$ (mm)
R1	17.95	3.24	4.11
R2	15.83	1.53	2.18
SP1	29.51	7.89	18.11
SP2	31.01	9.34	15.13
SA1	31.68	6.52	10.09
SA2	31.64	5.83	11.06

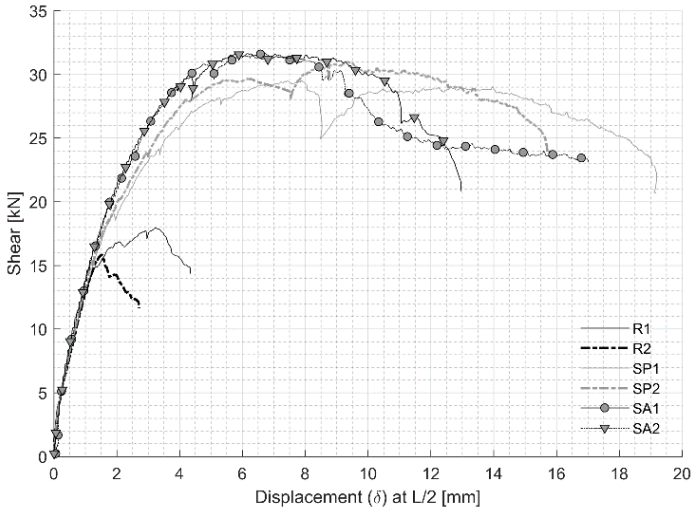

Figure 9. Shear-displacement curve of all reported tests.

The failure mechanism of the reference beams (R1 and R2) is characterized by the presence of a well-defined critical crack (see Figure 10), and it is different to the observed crack pattern on the strengthened specimens: cracks are more inclined and distributed along the beam length. Therefore, by strengthening the beams it has been possible to increase the shear strength and to change the failure mechanism, from shear to a mixed flexure-shear failure (with compression chord failure). In the beams with non-activated strips (SP1 and SP2) it is appreciated a more evident crack pattern than in beams with the activated strips (SA1 and SA2). However, the fact that this first series of tests had a flexural, or mixed flexural-shear failure mode, has not permitted to observe an evident difference of the ultimate state of the critical shear on the differently strengthened beams (with and without activation). New tests in the lab are looking for shear failures on the strengthened beams, which is necessary to be able to evaluate the strengthening efficiency, although it is not a desirable situation in real engineering. By using DIC it can be appreciated that, in the case of beams with activated strips (SA1 and SA2, Fig. 12) the shear cracks appear closer to the load application point, compared to the case of the retrofitted beams without activation (SP1 and SP2, Fig. 12) in which the shear cracks are more distributed along the length of the specimens.

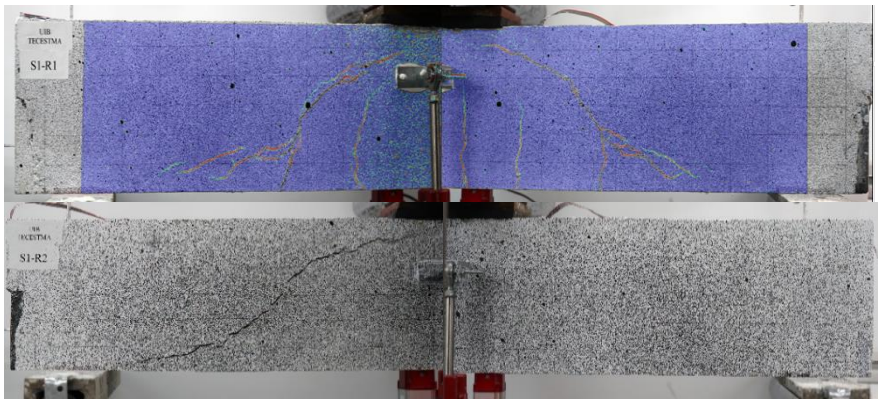

Figure 10. State of the reference beams, R1 and R2, after the peak load.

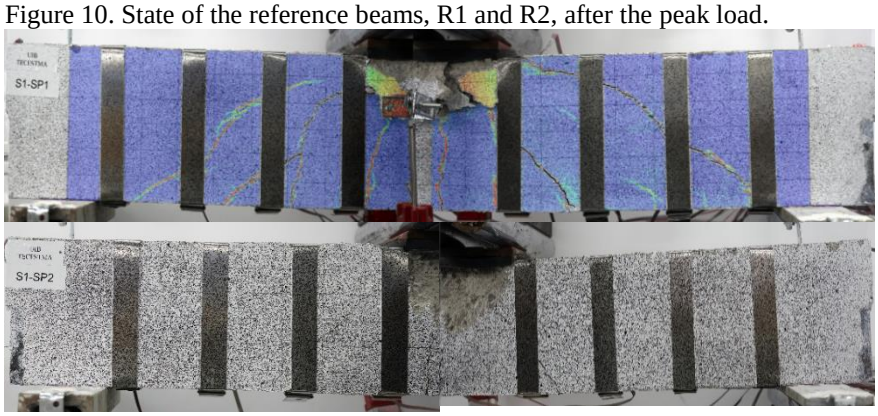

Figure 11. State of the non-actively strengthened beams, SP1 and SP2, after the peak load.

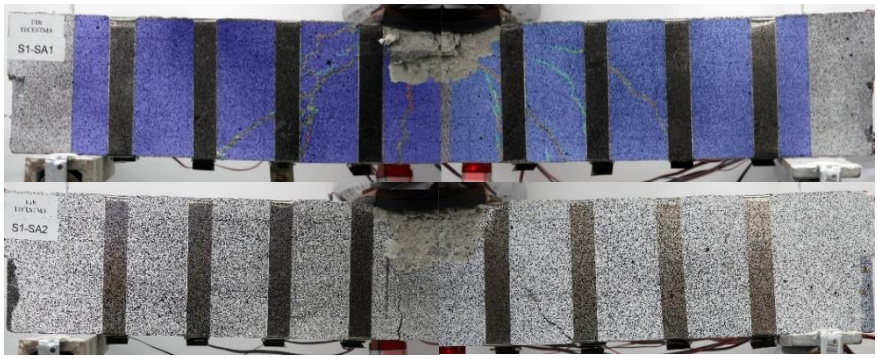

Figure 12. State of the actively strengthened beams, SA1/SA2, after the peak load.

5 FUTURE RESEARCH

The application of Fe-SMA strips as shear strengthening on reinforced concrete beams has been validated in this preliminary experimental campaign. The research continues to validate different layouts, different anchorage techniques, and the study of different mechanical models for its practical application in structural design. The tests on small-scale concrete beams were analyzed in detail with digital image correlation for an ongoing research project in order to evaluate the crack pattern evolution and to study the relevance of the different transfer actions considered in different shear mechanical models. Nonlinear finite element models, including the particularities of the SMAs, are being developed in ATENA software with the aim to perform a more complete analysis of the structural response and behavior of the tested specimens. Finally,

real-scale reinforced concrete beams, with internal conventional stirrups and external strengthening strips, are being tested at this moment to validate the technology in more realistic conditions.

6 CONCLUSIONS

This communication has presented the preliminary results of a more complex experimental campaign. The results show that the beams strengthened with Fe-SMA strips demonstrated an increase of the strength and ductility with respect to the un-strengthened beam: the failure mechanism changed from a brittle shear failure to a flexural failure. The strengthening methodology has been applied with and without activation to compare the benefits and differences. The variation of the modulus of elasticity of the strengthening material has been clearly shown. Another important issue is that the recovering shape of this material is lower than that of others SMA. Thus, the application of this technology should be done carefully, to avoid any gap between the beam and the strips, which could lead to a significant reduction of recovery stresses. Finally, the experimental tests on small-scale concrete beams were analyzed in detail with digital image correlation. The no appearance of shear cracks close to the supports in the case of the beams retrofitted with active strips shows that the confinement is effective with the activation of the Fe-SMA strips.

7 ACKNOWLEDGEMENTS

This research was developed in the framework of the project HORVITAL-sp2 “Development of strengthening techniques with advanced materials for concrete structures and their mechanical behavior models to extend their lifetime” - BIA2015-64672-C4-3-R (AEI – FEDER, UE). The authors appreciate the contribution of re-fer AG Strengthening Solution Company, which provided the Fe-SMA strips.

8 REFERENCES

Augenti, N. & Parisi, F., “Learning from construction failures due to the 2009 L'Aquila, Italy, earthquake”, J. Perform. Constr. Facil., 24, 2010, pp. 536–555.

Cladera, A. et al., “Iron-based shape memory alloys for civil engineering structures: An overview”, Construction and Building Materials, 63, 2014, pp.281–93.

Czaderski, C. et al., “Feasibility of iron-based shape memory alloy strips for prestressed strengthening of concrete structures”, Construction and Building Materials, 56, 2014, pp.94–105.

Derkowski, W., “Opportunities and risks araising from the properties of FRP materials used for structural strengthening”. Procedia Engineering, 108, 2015, pp.371-79.

Dong, Z. et al., “A Novel Fe-Mn-Si Shape Memory Alloy With Improved Shape Recovery Properties by VC Precipitation”, 11(2), 2009, pp.40-44.

Lee, W.J. et al., “Stress recovery behavior of an Fe-Mn-Si-Cr-Ni-VC shape memory alloy used for prestressing”. Smart Material and Structures, 2013, 22(12).

Ruiz-Pinilla, J.G. et al., "Learning from RC Building Structures Damaged by the Earthquake in Lorca, Spain, in 2011". Engineering Failure Analysis, 68, 2016, pp. 76-86.

Shahverdi, M., Czaderski, C. & Motavalli, M., “Iron-based shape memory alloys for prestressed near-surface mounted strengthening of reinforced concrete beams” Construction and Building Materials, 112, 2016, pp.28–38.